THE GEOLOGICAL SOCIETY OF AMERICA®

Rapid variation in upper-mantle rheology across the San Andreas fault system and Salton Trough, southernmost California, USA

Shahar Barak* and Simon L. Klemperer
Department of Geophysics, Stanford University, 397 Panama Mall, Stanford, California 94305, USA

ABSTRACT

We present new shear-wave splitting data showing systematic lateral variations in upper-mantle anisotropy across the plate boundary in southernmost California (USA). Beneath the Peninsular Ranges batholith, fast polarization directions parallel the direction of former Farallon subduction, suggestive of a slab remnant. Near the eastern edge of the batholith, across the Elsinore fault, fast polarization directions change rapidly to align with the direction of San Andreas fault shear. We infer that the Elsinore fault penetrates the entire lithosphere and may represent a future localization of the plate boundary that is migrating west from the San Andreas fault. Beneath the Salton Trough and the Chocolate Mountains region, large splitting times, despite a very thin lithosphere, imply vertical melt pockets in the uppermost mantle aligned in the shear direction. Largest splitting times, ~1.2 s, are seen closest to the Sand Hills fault that projects southeast from the San Andreas fault. Further east, in the southern Basin and Range province, fast directions align with North America absolute plate motion.

INTRODUCTION

Analysis of teleseismic shear-wave splitting is a standard tool for studying upper-mantle anisotropy created by strain-induced lattice-preferred orientation of minerals or by preferentially oriented melt-filled inclusions, and hence also for studying changes in rheology (e.g., Savage, 1999, and references therein). A shear wave passing through an anisotropic medium splits into slow and fast waves with orthogonal polarizations. Two splitting parameters (polarization, φ, and delay time, δt) provide a direct estimate of the axis and magnitude of the anisotropy for simple cases and show systematic variations with back-azimuth to the source earthquake in more complex scenarios.

Despite Southern California's (USA) complex tectonic history and active plate boundary oriented northwest-southeast (e.g., Dickinson, 2008, 2009; Barak et al., 2015) (Fig. 1A), previous studies of shear-wave splitting in Southern California (e.g., Polet and Kanamori, 2002; Kosarian et al., 2011) show a nearly uniform fast axis of anisotropy oriented approximately west-east (Fig. 1C). This has been interpreted as due to inherited North America plate motion (Kosarian et al., 2011), pre–late Cenozoic compression (Polet and Kanamori, 2002), or mantle flow around the southern edge of the subducting Gorda slab (Zandt and Humphreys, 2008). The same general west-east pattern continues to the southern tip of Baja California (Mexico), west and east of the Gulf of California rift margins (Long, 2010; Fig. 1A). Recent three-dimensional (3-D) tomographic inversion of shear-wave splitting measurements, despite the previous scarcity of data in southernmost California, has begun to suggest complicated structure, including a northwest fast axis of anisotropy in the Salton Trough (ST) (Monteiller and Chevrot, 2011) where Gulf of California ocean spreading propagates into continental crust along the San Andreas fault (Elders et al., 1972).

Here we analyze shear-wave splitting measurements on our array of 48 seismometers that spanned southernmost California from A.D. 2011 to

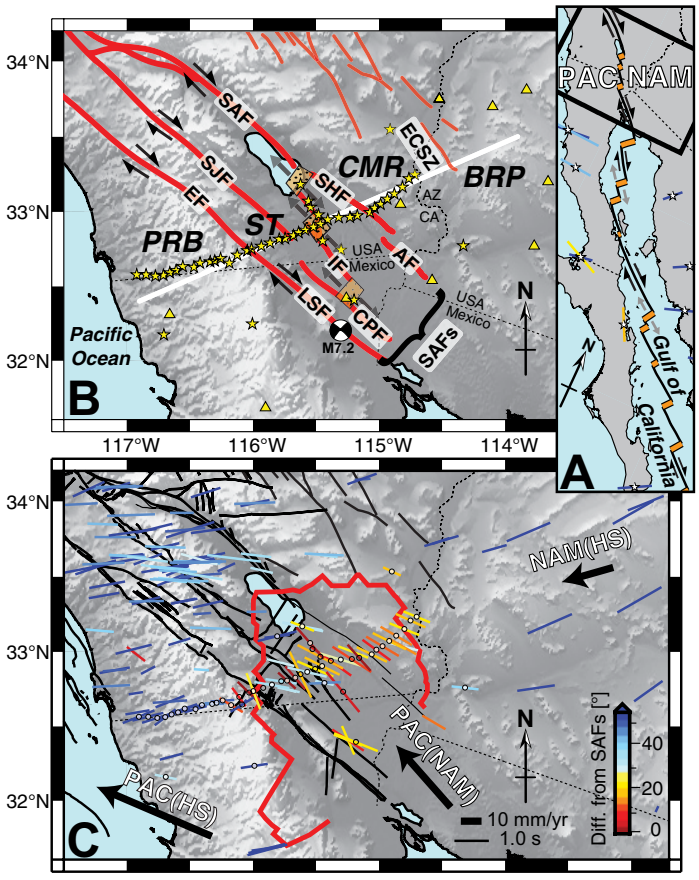

Figure 1. A: Pacific (PAC)–North America (NAM) plate boundary (black—transform; orange—spreading center), showing location of B and C (black rectangle), and shear-wave splitting (SWS) fast polarizations further south in Mexico (Long, 2010) using length scale and color scale as in C. B: Shaded-relief topography overlain with our seismic stations (stars), other permanent stations shown in Figure 2 (triangles), and line of section in Figure 2 (white line). BRP—southern Basin and Range province; CMR—Chocolate Mountains region; PRB—Peninsular Ranges batholith; ST—Salton Trough. Dot-patterned orange boxes show active spreading centers (Elders et al., 1972). Strike-slip focal mechanism: 4 April 2010 El Mayor–Cucapah earthquake. Thick red lines show major faults of San Andreas fault system (SAFs) (AF—Algodones; CPF—Cerro Prieto; EF—Elsinore; IF—Imperial; LSF—Laguna Salada; SAF—San Andreas; SHF—Sand Hills; SJF—San Jacinto). Thin red lines show southeast extension of Eastern California Shear Zone (ECSZ) (Darin and Dorsey, 2013). C: SWS fast polarizations with lengths proportional to delay time (colored bars). This study: white circles (open circles if no "good" or "fair" results were available); other SWS results: Wüstefeld et al. (2009); Liu et al. (2014; only "A" quality data, weighted by their standard deviation). Color of bars indicates difference in degrees from trend of SAFs. Black arrows are plate-motion vectors relative to fixed-hotspot (HS) frame (Gripp and Gordon, 2002). Red line is 55 km depth contour of lithosphere-asthenosphere boundary (Lekic et al., 2011). Thin black lines are fault traces (Plesch et al., 2007).

*Current address: Noble Energy, Houston, Texas 77070, USA.

2013 (Barak et al., 2015; Fig. 1B). We show systematic lateral variations in anisotropy between different geologic regions. Our data suggest new constraints on the underlying upper-mantle rheology and implications for active tectonics and associated earthquake hazard.

ANALYSIS OF SHEAR-WAVE SPLITTING MEASUREMENTS

We use SplitLab software (Wüstefeld et al., 2008) to determine splitting parameters (φ, δt) for SKS and SKKS phases from earthquakes with $M \geq 6.0$ at epicentral distances of 84°–184° (see Fig. DR1 in the GSA Data Repository[1]). These phases, radially polarized at the core-mantle boundary, are only affected by anisotropy beneath the station, and their steep ascent through the mantle provides good lateral resolution. For each measurement we assign a quality: good, fair, or poor (Figs. DR2–DR5). We do not entirely discard poor measurements because a few stations have only poor measurements, yet averaged results from these stations are still consistent with adjacent stations (Fig. 1B). For the four permanent stations in the ST common to our study and that of Monteiller and Chevrot (2011), who used a different analysis method, the fast polarization directions match within error (Table DR2 in the Data Repository). For each station we search for a best-fitting model with two layers of horizontal anisotropy, but also calculate a quality-weighted average φ and δt for the best-fitting one-layer model (see the Data Repository for details).

RESULTS

Despite modest variation in splitting parameters with back-azimuth at all of our stations (Figs. DR6–DR55), our data are best modeled by a single layer with horizontal anisotropy, as also indicated by 3-D models that show a largely constant shear-wave polarization with depth in the ST region (Monteiller and Chevrot, 2011). Our one-layer model assumption is supported by the lateral consistency of our station-averaged splitting results and their correlation with other seismic observations (Lekic et al., 2011; Barak et al., 2015; Fig. 2; Fig. DR2). We observe systematic variations in station-averaged fast directions along our 250 km, WSW-ENE–trending array (Fig. 1). We divide our stations into four geographical groups, correlated with different geologic regions that are distinguished by different mean values of φ and δt, hereafter φ_m and δt_m (Fig. 2A; Fig. DR2; Table DR1). Across the Peninsular Ranges batholith (PRB), which is now part of the Pacific plate, φ_m is ~079°, orthogonal to the strike of the batholith, and δt_m is ~0.8 s. Close to the Elsinore fault (EF), φ_m changes rapidly (over <10 km at the surface) from 079° outside the ST to 124° within the trough. δt_m is ~1.0 s, but δt gradually increases to 1.3 s across the ST (Figs. 1 and 2A; Fig. DR2). The 124° fast polarization is almost parallel to the EF (trend 130°) and the Sand Hills fault (SHF) (trend 135°). Northwest fast polarizations are also evident at the handful of other stations in the ST north and south of the U.S.-Mexico border (Table DR1) (Fig. 1). Northeast of the SHF, across the Chocolate Mountains region (CMR) to the Colorado River and the southeastern continuation of the Eastern California Shear Zone (ECSZ), fast directions continue to rotate very slightly counterclockwise, and δt gradually decreases to 0.8 s. Across the southeast projection of the ECSZ, a second large change in fast direction occurs over <20 km at the surface, and possibly over <10 km, albeit less well-constrained than the change near the EF because of our dispersed station geometry. In this eastern Basin and Range province domain, δt_m is ~1.0s and φ_m is ~076°, sub-parallel to the 074° absolute plate motion of North America in a hotspot reference frame [NAM(HS)] (Figs. 1C and 2A; Fig. DR2).

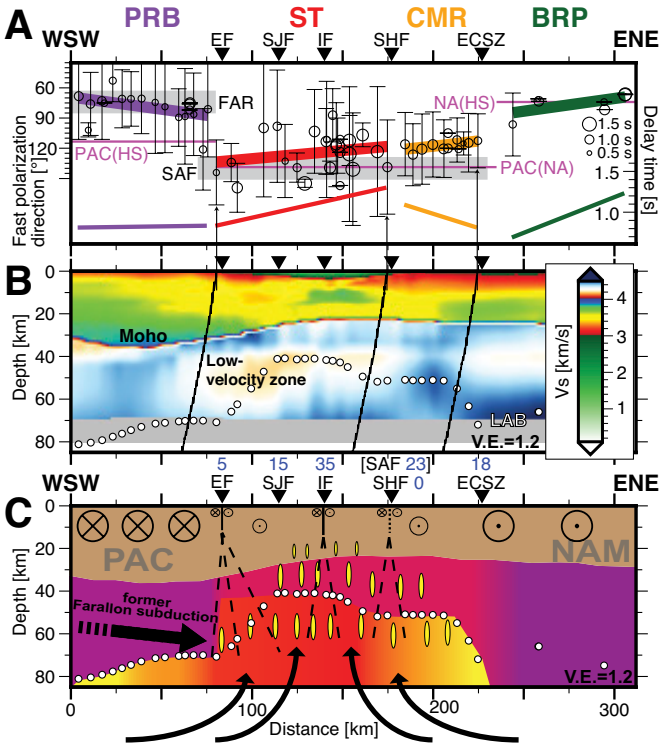

Figure 2. A: Our shear-wave splitting results and ten previous measurements (Fig. 1B), projected onto profile shown by white line in Figure 1B. Thick and thin solid colored lines are least-squares linear fits to split directions (φ) and split times (δt), respectively, for each group of stations (Peninsular Ranges batholith [PRB], Salton Trough [ST], Chocolate Mountains region [CMR], southern Basin and Range province [BRP]). Error bars are quality-weighted standard deviation of polarization direction; circle diameters are proportional to split time. Thin horizontal magenta lines show Pacific and North America absolute [PAC(HS), NAM(HS); HS refers to hotspot reference frame] and relative [PAC(NA)] plate motions. Thick gray bars show Farallon (FAR) motion with respect to North America plate, and strike of San Andreas fault system (faults: EF—Elsinore; SJF—San Jacinto; IF—Imperial; SHF—Sand Hills; SAF—San Andreas; ECSZ—Eastern California Shear Zone). B: S-velocity model (color scale) (Barak et al., 2015) overlain with lithosphere-asthenosphere boundary (LAB) from Sp receiver functions (white circles; Lekic et al., 2011). Black lines are example SKS ray-paths, using mean event azimuth, distance, and depth. V.E.—vertical exaggeration. C: Tectonic cartoon. Blue numbers above fault abbreviations are maximum estimates of geodetic fault slip rates (in mm/yr) (Chuang and Johnson, 2011; Field et al., 2013). Yellow ovals are aligned melt channels. Curved arrows show upwelling mantle. Dashed lines are inferred shear zones. ⊗ and ⊙ are block motions into and out of page, respectively, with size crudely scaled to velocity with respect to Elsinore fault.

DISCUSSION

Shear-wave splitting is commonly ascribed either to vertically coherent deformation in which anisotropy from the last significant tectonic episode recorded in the crust is also preserved in the mantle lithosphere, or to asthenospheric flow for which the associated anisotropy is governed by absolute plate motions (e.g., Savage, 1999). In our study area, we expect the common A-type (or D- or E-type) olivine fabrics that produce shear-parallel polarization of the fast directions, and not B or C types that require much higher water content and/or much higher stress than expected in the shallow mantle of Southern California (Karato et al., 2008).

The PRB, a Mesozoic magmatic arc formed above the subducting Farallon plate (e.g., Dickinson, 2008, 2009), has φ_m of ~079°, oriented 34° counterclockwise from the Pacific absolute plate motion [PAC(HS) = 293°], thereby excluding asthenospheric flow due to Pacific absolute

[1]GSA Data Repository item 2016190, Figures DR1–DR55, Tables DR1 and DR2, descriptions of Data Sets DR1 and DR2, and two ASCII files containing Data Sets DR1 and DR2, is available online at www.geosociety.org/pubs/ft2016.htm, or on request from editing@geosociety.org or Documents Secretary, GSA, P.O. Box 9140, Boulder, CO 80301, USA.

plate motion as the cause of the anisotropy. Our observed fast directions, as well as others in the PRB north and south of the U.S.-Mexico border (Figs. 1A and 1C), are ubiquitously orthogonal to the strike of the batholith (Fig. 1) and are aligned with both the NAM(HS) absolute plate motion (074°) and the Farallon–North America convergence direction of 70°–80° (Atwater and Stock, 1998). Although the batholith was formerly part of North America, it lay directly above the subducting Farallon plate, so would not likely have acquired anisotropy due to asthenospheric flow associated with the NAM(HS) absolute plate motion. The 70–80-km-thick lithosphere of the PRB (Lekic et al., 2011) (Fig. 2B) is sufficient to develop the observed 0.8 s delay time, under the assumption of an ~10-km-thick mid-lower crustal layer with average anisotropy of ~10% (Porter et al., 2011) and up to 5% anisotropy in the mantle lithosphere, as commonly found in mantle xenoliths (e.g., Savage, 1999). Hence "frozen-in" lithospheric fabric aligned in the direction of subduction is the likely cause of the dominant west-east fast direction observed along the entire 1200 km length of the batholith (Fig. 1A). It is controversial whether the high-velocity upper mantle and lower crust of the PRB represents the magmatic arc or underthrust Farallon slab (Barak et al., 2015). The high anisotropy and relatively low upper-mantle shear velocities (Barak et al., 2015) are both more consistent with peridotite than with eclogite (Worthington et al., 2013), so we favor the interpretation of a slab remnant (cf. Wang et al., 2013). The 6 m.y. elapsed since the transform plate boundary migrated inboard of Baja California to the modern San Andreas fault system (SAFs), transferring the PRB to the Pacific plate (Stock and Hodges, 1989), must be insufficient—as modeled by Savage et al. (2004)—to have rotated an older west-east anisotropic fabric to be parallel to the fault system or to the Pacific absolute plate motion (Fig. 1B).

At the eastern edge of the PRB, fast directions rapidly rotate to a northwest-southeast direction over a distance of <10 km. Our 120-km-wide region of unexpected northwest-oriented fast S-wave polarizations in the ST correlates spatially with a region of upwelling magma (Barak et al., 2015) beneath a lithosphere as thin as 40 km (Lekic et al., 2011) (Fig. 2B). The thin lithosphere is bounded by rapid lateral increases in lithospheric thickness coincident with the boundaries implied by our splitting measurements, close to the EF and the southern extension of the ECSZ (Fig. 1B). Inward mantle flow (perpendicular to the SAF) due to lithospheric thinning beneath the ST would produce a fast direction orthogonal to the north-northeast–elongate trough and Gulf of California, which we do not observe. Instead, the northwest fast axis—parallel to the SAFs—suggests that mantle flow beneath the rift is dominated by shearing motion in this oblique-transform plate boundary, as also expressed in the crust by the very long transform faults connecting the very short spreading centers (Elders et al., 1972) (Fig. 1A). The rapid lateral variation in anisotropy confines the cause of anisotropy to shallow levels, certainly above 90 km depth given our seismic waves of ~8 s period (e.g., Hammond et al., 2010). Nonetheless, despite the shallow source, we observe ~1.0 s of splitting delay time (Fig. 2A; Fig. DR2). Crustal anisotropy typically contributes only 0.1–0.3 s (e.g., Savage, 1999). Even the 1% melt organized in lower-crustal melt channels that is permitted by our velocity tomography (Barak et al., 2015) only contributes 0.25 s splitting for an aspect ratio of 0.01 (Ayele et al., 2004). The mantle lithosphere beneath the ST is so thin, just 10–15 km thick beneath the region of largest splitting times (Lekic et al., 2011; Barak et al., 2015) (Figs. 2B and 1C), that shearing would only produce <0.2 s splitting given typical anisotropy of sheared mantle xenoliths of <5% (e.g., Savage, 1999). Therefore, to explain the large split times, we argue that vertical melt-filled channels must be present in the mantle (Ayele et al., 2004; Hammond et al., 2010; Holtzman and Kendall, 2010), aligned in the transform shear direction (northwest-southeast) and orthogonal to the direction of least principal stress. Oblique rift systems can exhibit a difference in dike orientation between the crust and the mantle (Abelson and Agnon, 1997). Injection of melt into the crust over short elastic time scales results in dikes oriented orthogonal to the shear plane to minimize shear on their walls. In contrast, upper-mantle melt conduits form continuously in a ductile flow regime that reduces effective viscosity (Holtzman and Kendall, 2010), relaxes lithospheric stresses, and results in shear-parallel dikes regardless of the oblique divergence of the overlying plates (Abelson and Agnon, 1997). Assuming that the onset of melt occurs at depths of ~70 km (Wang et al., 2009; Lekic et al., 2011), a 30-km-thick layer with 1% melt organized in dikes, as inferred from our tomography (Barak et al., 2015), contributes 1 s split time for a 0.01 aspect ratio (Ayele et al., 2004).

The rapid change in fast direction across the EF can be modeled as due to a laterally varying viscosity structure (Savage et al., 2004; Bonnin et al., 2012) in which the greatest strain is concentrated within a low-viscosity region to the east (Pollitz et al., 2012). Because our SKS raypaths are mostly from the west and southwest, our stations are mapping anisotropic fabric development as much as 25 km southwest of the fault at 50 km depth, within the mantle lithosphere (Fig. 2B). There is no evidence that the EF dips southwest through the crust (Plesch et al., 2007; Barak et al., 2015), but our velocity model (Fig. 2B) and common conversion-point image (Fig. DR2) show that the upper-mantle low-velocity zone extends west beneath the fault, suggesting gradual heating of the cold PRB–Pacific plate by hot ST mantle. Because western strands of the SAFs are younger (Elsinore and San Jacinto faults: 1.1–1.3 Ma, Dorsey and Langenheim, 2015; SAF: >5.5 Ma, Stock and Hodges, 1989), we suggest that the plate boundary is migrating west to the EF (Fig. 2C). Westward migration has been previously inferred in the ST (Barak et al., 2015) and the northern Gulf of California (Aragón-Arreola and Martin-Barajas, 2007).

Mean splitting parameters barely change from the ST to the CMR (ST: φ_m ~124°, δt_m ~1.0 s; CMR: φ_m ~117°, δt_m ~0.9 s). However, these averages mask a significant change in split times, from δt of ~0.9 s at the EF to δt of ~1.3 s at the SHF, then a decrease back to δt ~0.8 s at the ECSZ (Fig. 2A; Fig. DR2). Because the lithosphere is almost as thin beneath the CMR as beneath the ST (Fig. 2B), there must still be a large contribution from the asthenosphere northeast of the SHF to account for the 0.9 s delay time. Hence, vertical melt inclusions likely also exist beneath the CMR, largely rotated into alignment with the plate-boundary SAFs shearing direction. The maximum split times are beneath the Sand Hills fault, the projection of the SAF that was the longest-lived locus of plate-boundary transform motion within the SAFs. A similar magnitude of decreasing delay times away from the SAF has been modeled in Northern California (Bonnin et al., 2012).

Within the southern Basin and Range province, φ_m (~076°) is aligned with the local NAM(HS) absolute plate motion (074°), suggesting shear at the lithosphere-asthenosphere boundary likely complemented by extensional vertically coherent deformation.

CONCLUSIONS

The distributed plate boundary in southernmost California coincides with an unusually weak uppermost mantle of melt-lubricated asthenosphere. Thermally controlled upper-mantle viscosity helps to localize deformation and strongly affects brittle deformation at the surface (Molnar, 1992). A large discrepancy between slip rates calculated using one-dimensional viscosity models and those measured by GPS stations and geologic data in and around the Salton Trough is unparalleled elsewhere in California (Chuang and Johnson, 2011; Field et al., 2013). The rapid lateral changes in viscosity we infer across the Elsinore fault and the Eastern California Shear Zone, previously only conjectured from satellite geodesy (Pollitz et al., 2012), should inform future inversions of slip rate, estimates of earthquake hazard, and understanding of geologic evolution.

ACKNOWLEDGMENTS

We thank C. Castillo, S. Chevrot, V. Langenheim, K. Liu, W. Thatcher, and an anonymous reviewer for valuable comments. Our seismic data are available from the Incorporated Research Institutions for Seismology Data Management Center (http://ds.iris.edu/ds/nodes/dmc/). This work was funded by National Science Foundation Geophysics program grant 0911743.

REFERENCES CITED

Abelson, M., and Agnon, A., 1997, Mechanics of oblique spreading and ridge segmentation: Earth and Planetary Science Letters, v. 148, p. 405–421, doi:10.1016/S0012-821X(97)00054-X.

Aragón-Arreola, M., and Martin-Barajas, A., 2007, Westward migration of extension in the northern Gulf of California, Mexico: Geology, v. 35, p. 571–574, doi:10.1130/G23360A.1.

Atwater, T., and Stock, J., 1998, Pacific–North America plate tectonics of the Neogene southwestern United States: An update: International Geology Review, v. 40, p. 375–402, doi:10.1080/00206819809465216.

Ayele, A., Stuart, G., and Kendall, J.-M., 2004, Insights into rifting from shear wave splitting and receiver functions: An example from Ethiopia: Geophysical Journal International, v. 157, p. 354–362, doi:10.1111/j.1365-246X.2004.02206.x.

Barak, S., Klemperer, S.L., and Lawrence, J.F., 2015, San Andreas Fault dip, Peninsular Ranges mafic lower-crust and partial melt in the Salton Trough, Southern California, from ambient-noise tomography: Geochemistry Geophysics Geosystems, v. 16, p. 3946–3972, doi:10.1002/2015GC005970.

Bonnin, M., Tommasi, A., Hassani, R., Chevrot, S., Wookey, J., and Barruol, G., 2012, Numerical modelling of the upper-mantle anisotropy beneath a migrating strike-slip plate boundary: The San Andreas Fault system: Geophysical Journal International, v. 191, p. 436–458, doi:10.1111/j.1365-246X.2012.05650.x.

Chuang, R.Y., and Johnson, K.M., 2011, Reconciling geologic and geodetic model fault slip-rate discrepancies in Southern California: Consideration of nonsteady mantle flow and lower crustal fault creep: Geology, v. 39, p. 627–630, doi:10.1130/G32120.1.

Darin, M.H., and Dorsey, R.J., 2013, Reconciling disparate estimates of total offset on the southern San Andreas fault: Geology, v. 41, p. 975–978, doi:10.1130/G34276.1.

Dickinson, W.R., 2008, Accretionary Mesozoic–Cenozoic expansion of the Cordilleran continental margin in California and adjacent Oregon: Geosphere, v. 4, p. 329–353, doi:10.1130/GES00105.1.

Dickinson, W.R., 2009, Anatomy and global context of the North American Cordillera, *in* Kay, S.M., et al., eds., Backbone of the Americas: Shallow Subduction, Plateau Uplift, and Ridge and Terrane Collision: Geological Society of America Memoir 204, p. 1–29, doi:10.1130/2009.1204(01).

Dorsey, R.J., and Langenheim, V.E., 2015, Crustal-scale tilting of the central Salton block, southern California: Geosphere, v. 11, p. 1365–1383, doi:10.1130/GES01167.1.

Elders, W.A., Rex, R.W., Robinson, P.T., Biehler, S., and Meidav, T., 1972, Crustal spreading in southern California: The Imperial Valley and the Gulf of California formed by the rifting apart of a continental plate: Science, v. 178, p. 15–24, doi:10.1126/science.178.4056.15.

Field, E.H., et al., 2013, Uniform California earthquake rupture forecast, version 3 (UCERF3)—The time-independent model: U.S. Geological Survey Open-File Report 2013-1165, 97 p., doi:10.3133/ofr20131165.

Gripp, A.E., and Gordon, R.G., 2002, Young tracks of hotspots and current plate velocities: Geophysical Journal International, v. 150, p. 321–361, doi:10.1046/j.1365-246X.2002.01627.x.

Hammond, J.O.S., Kendall, J.-M., Angus, D., and Wookey, J., 2010, Interpreting spatial variations in anisotropy: Insights into the Main Ethiopian Rift from SKS waveform modelling: Geophysical Journal International, v. 181, p. 1701–1712, doi:10.1111/j.1365-246X.2010.04587.x.

Holtzman, B.K., and Kendall, J.-M., 2010, Organized melt, seismic anisotropy, and plate boundary lubrication: Geochemistry Geophysics Geosystems, v. 11, Q0AB06, doi:10.1029/2010GC003296.

Karato, S., Jung, H., Katayama, I., and Skemer, P., 2008, Geodynamic significance of seismic anisotropy of the upper mantle: New insights from laboratory studies: Annual Review of Earth and Planetary Sciences, v. 36, p. 59–95, doi:10.1146/annurev.earth.36.031207.124120.

Kosarian, M., Davis, P.M., Tanimoto, T., and Clayton, R.W., 2011, The relationship between upper-mantle anisotropic structures beneath California, transpression, and absolute plate motions: Journal of Geophysical Research, v. 116, B08307, doi:10.1029/2010JB007742.

Lekic, V., French, S.W., and Fischer, K.M., 2011, Lithospheric thinning beneath rifted regions of Southern California: Science, v. 334, p. 783–787, doi:10.1126/science.1208898.

Liu, K.H., Elsheikh, A., Lemnifi, A., Purevsuren, U., Ray, M., Refayee, H., Yang, B.B., Yu, Y., and Gao, S.S., 2014, A uniform database of teleseismic shear-wave splitting measurements for the western and central United States: Geochemistry Geophysics Geosystems, v. 15, p. 2075–2085, doi:10.1002/2014GC005267.

Long, M.D., 2010, Frequency-dependent shear wave splitting and heterogeneous anisotropic structure beneath the Gulf of California region: Physics of the Earth and Planetary Interiors, v. 182, p. 59–72, doi:10.1016/j.pepi.2010.06.005.

Molnar, P., 1992, Brace-Goetze strength profiles, the partitioning of strike-slip and thrust faulting at zones of oblique convergence, and the stress–heat flow paradox of the San Andreas fault, *in* Evans, B., and Wong, T.F., eds., Fault Mechanics and Transport Properties of Rocks: San Diego, California, Academic Press, p. 435–459, doi:10.1016/S0074-6142(08)62833-8.

Monteiller, V., and Chevrot, S., 2011, High-resolution imaging of the deep anisotropic structure of the San Andreas Fault system beneath southern California: Geophysical Journal International, v. 186, p. 418–446, doi:10.1111/j.1365-246X.2011.05082.x.

Plesch, A., et al., 2007, Community fault model (CFM) for Southern California: Bulletin of the Seismological Society of America, v. 97, p. 1793–1802, doi:10.1785/0120050211.

Polet, J., and Kanamori, H., 2002, Anisotropy beneath California: Shear wave splitting measurements using a dense broadband array: Geophysical Journal International, v. 149, p. 313–327, doi:10.1046/j.1365-246X.2002.01630.x.

Pollitz, F.F., Bürgmann, R., and Thatcher, W., 2012, Illumination of rheological mantle heterogeneity by the M7.2 2010 El Mayor–Cucapah earthquake: Geochemistry Geophysics Geosystems, v. 13, Q06002, doi:10.1029/2012GC004139.

Porter, R., Zandt, G., and McQuarrie, N., 2011, Pervasive lower-crustal seismic anisotropy in Southern California: Evidence for underplated schists and active tectonics: Lithosphere, v. 3, p. 201–220, doi:10.1130/L126.1.

Savage, M.K., 1999, Seismic anisotropy and mantle deformation: What have we learned from shear wave splitting?: Reviews of Geophysics, v. 37, p. 65–106, doi:10.1029/98RG02075.

Savage, M.K., Fischer, K.M., and Hall, C.E., 2004, Strain modelling, seismic anisotropy and coupling at strike-slip boundaries: Applications in New Zealand and the San Andreas fault, *in* Grocott, J., et al., eds., Vertical Coupling and Decoupling in the Lithosphere: Geological Society of London Special Publication 227, p. 9–39, doi:10.1144/GSL.SP.2004.227.01.02.

Stock, J.M., and Hodges, K.V., 1989, Pre-Pliocene extension around the Gulf of California and the transfer of Baja California to the Pacific plate: Tectonics, v. 8, p. 99–115, doi:10.1029/TC008i001p00099.

Wang, Y., Forsyth, D.W., and Savage, B., 2009, Convective upwelling in the mantle beneath the Gulf of California: Nature, v. 462, p. 499–501, doi:10.1038/nature08552.

Wang, Y., Forsyth, D.W., Rau, C.J., Carriero, N., Schmandt, B., Gaherty, J.B., and Savage, B., 2013, Fossil slabs attached to unsubducted fragments of the Farallon plate: Proceedings of the National Academy of Sciences of the United States of America, v. 110, p. 5342–5346, doi:10.1073/pnas.1214880110.

Worthington, J.R., Hacker, B.R., and Zandt, G., 2013, Distinguishing eclogite from peridotite: EBSD-based calculations of seismic velocities: Geophysical Journal International, v. 193, p. 489–505, doi:10.1093/gji/ggt004.

Wüstefeld, A., Bokelmann, G., Zaroli, C., and Barruol, G., 2008, SplitLab: A shear-wave splitting environment in Matlab: Computers & Geosciences, v. 34, p. 515–528, doi:10.1016/j.cageo.2007.08.002.

Wüstefeld, A., Bokelmann, G., Barruol, G., and Montagner, J.-P., 2009, Identifying global seismic anisotropy patterns by correlating shear-wave splitting and surface-wave data: Physics of the Earth and Planetary Interiors, v. 176, p. 198–212, doi:10.1016/j.pepi.2009.05.006.

Zandt, G., and Humphreys, E., 2008, Toroidal mantle flow through the western U.S. slab window: Geology, v. 36, p. 295–298, doi:10.1130/G24611A.1.

Manuscript received 28 February 2016
Revised manuscript received 21 May 2016
Manuscript accepted 24 May 2016

Printed in USA